Icarus 205 (2010) 619–626

Contents lists available at ScienceDirect

Icarus

journal homepage: www.elsevier.com/locate/icarus

R-band light curve of Comet 9P/Tempel 1 during the Deep Impact event

Tyler R. Mitchell [a,*], William F. Welsh [b], Paul B. Etzel [b], Robert J. Barber [c], Steve Miller [c], Tom S. Stallard [d], Jonathan Tennyson [c]

[a] Department of Astrophysical and Planetary Sciences, University of Colorado, Boulder, CO 80309-0391, USA
[b] Department of Astronomy, San Diego State University, San Diego, CA 92182, USA
[c] Department of Physics and Astronomy, University College London, London, WC1E 6BT, UK
[d] Department of Physics and Astronomy, University of Leicester, Leicester, LE1 7RH, UK

ARTICLE INFO

Article history:
Received 28 February 2008
Revised 27 July 2009
Accepted 27 July 2009
Available online 25 August 2009

Keywords:
Comets, Dust
Photometry

ABSTRACT

We present high-speed CCD photometry of Comet 9P/Tempel 1 during the *Deep Impact* event on 2005 July 4 UT. Approximately 2 h and 50 min of R-band data were acquired at Mount Laguna Observatory with a temporal resolution of 5.5 s. The flux increased by 9% in the first minute after impact. This was followed by a more gradual two-part linear rise, with a change in slope at 9.2 min post-impact, at which time the rate of brightening increased from ~3% min^{-1} to ~5% min^{-1}. An analysis of the light curve obtained with the guide camera on the United Kingdom Infrared Telescope and yields very similar results. These findings are mildly in disagreement with the 3-part linear rise found by Fernández et al. (2007) in that we do not find any evidence for a change at 4 min post-impact. We interpret the linear rise phase as due to solar illumination of the edge of an expanding optically thick dust ejecta plume. After approximately 20 min, the light curves begin to flatten out, perhaps coincident with the start of the transition to becoming optically thin. In the large apertures (>10″) the light curve continues to gradually rise until the end of the observations. In smaller apertures, the light curves reach a peak at approximately 50 min, then decrease back towards the pre-impact flux level. The drop in flux in the smaller apertures may be caused by the ejecta expanding beyond the edge of the photometric aperture, and if so, we can use this timescale to infer an expansion velocity of ~0.5 km s^{-1}, consistent with previous published estimates.

1. Introduction

Comet 9P/Tempel 1 was first discovered by Ernst Tempel in 1867 and belongs to the Jupiter-Family of short period comets with its 5.50 year orbital period (Marsden, 1983). Comet 9P/Tempel 1 has made many perihelion passages and spent a considerable amount of time in the inner Solar System, making it an excellent candidate for studying evolutionary change in the outer layers of comets.

On 2005 July 4 UT, the 370 kg "impactor" from the *Deep Impact* spacecraft successfully collided with Comet 9P/Tempel 1 (A'Hearn et al., 2005). At 05:44:36 UT, corresponding to an Earth-receive time of 5:52:02 UT, the comet was at a geocentric distance of approximately 0.894 AU as the impactor struck with a speed of ~10.3 km s^{-1} (A'Hearn et al., 2005). The impactor excavated ~10^4 metric tons of dust (Sugita et al., 2005) and 4.5×10^6 kg of water (Küppers et al., 2005). The resulting blast enabled an investigation of the chemical and physical composition of the comet.

The impact event was observed by an unprecedented world-wide multi-wavelength monitoring campaign. Observations began as early as 1997, continued for months following the impact event. In total, Comet 9P/Tempel 1 was observed with 73 professional telescopes at 35 observatories world-wide, along with many space-based instruments, for more than 550 nights (Meech et al., 2005). In Section 2 we give a description of the observations made at Mt. Laguna Observatory and the techniques used to calibrate of these data. In Section 3 we present an analysis of our light curve. Considerable effort is made to quantitatively compare our photometry with those obtained at IRFT and at UKIRT. This is particularly important given the unique nature of the Deep Impact experiment. We present an estimate of the ejecta velocity in Section 4, followed by a discussion and summary of our results in Sections 5 and 6.

2. Observations and data reduction

Images of 9P/Tempel 1 were obtained on the 1-m telescope at San Diego State University's Mount Laguna Observatory (MLO) using a Fairchild CCD and a Kron R-band filter. The liquid nitrogen cooled 2048^2 CCD was set up in a 2×2 binning mode with a sub-array of 200×200 pixels to enable high-speed readout. Four-second

* Corresponding author. Address: Department of Astrophysical and Planetary Sciences, University of Colorado, Campus Box 391, Boulder, CO 80309-0391, USA.
E-mail address: Tyler.R.Mitchell@colorado.edu (T.R. Mitchell).

0019-1035/$ - see front matter © 2009 Elsevier Inc. All rights reserved.
doi:10.1016/j.icarus.2009.07.046

exposures provided an average temporal resolution of 5.5 s. The expected need for such high temporal resolution was based on predictions that the comet could brighten from about 10th magnitude to as bright as 5th or 6th magnitude (Warner and Redfern, 2005). To make sure the CCD did not saturate, short exposures were taken; and to make sure the event was temporally resolved, short readout times were required. In actuality, the amount of material released as a result of the impact was similar to normal cometary outbursts and the brightening was relatively modest, and the cometary flux returned to pre-impact levels about a week after the impact (Küppers et al., 2005).

In 2×2 binning mode the CCD plate scale is $\sim 0.''8$ per pixel, with a resultant field of view of $2.7' \times 2.7'$. On the night of 2005 July 4 UT, observations began approximately 64 min before the impact and lasted for just under 107 min post-impact. Observations were also made for 1 h and a half on July 2 UT and for 3 h on July 3 and 5 UT. Here we present results only from data collected on the night of July 4 UT.

The conditions at MLO on July 4 were photometric with a seeing full-width-half-maximum (FWHM) of $2.75''$ at the time of impact and an average seeing of $2.8''$ for the entire evening. For comparison, the FWHM of the comet just prior to impact is $4.23''$. Fig. 1 shows the seeing FWHM during the observations. Four different (faint) stars were used because the motion of the comet eventually caused the comparison stars to drift off the field of view. The seeing remained $\sim 3''$ FWHM and fairly constant until $\sim$90 min post-impact (7:24 UT, indicated with the dotted line; this is at an airmass 5.9). To observe as much of the event as possible, data were collected up to an airmass of 8.6, but after 90 min the seeing increased noticeably and became highly variable, and the data are less trustworthy.

The diffuse nature of the comet's coma, the small field of view and our short exposure times, which produced a very low S/N in our field stars, led us to employ non-standard techniques in the removal of the sky background from our images. According to A'Hearn (1983), the sky around a comet should be measured several arcminutes away from the comet and in some cases up to a degree away. The small angular field of view of our images, required for fine temporal sampling, prevented this. Therefore, no annuli were used in subtracting out the sky brightness from the comet. Instead, the mode of the bottom quarter (lower 50 pixels) of each image was subtracted from the entire image. The bottom of each image was chosen because the comet is located in the center of each frame with the coma and tail extending towards the upper-left (SE). Fig. 2, a cut from our first image at 4:48:10 UT, shows a single CCD column containing the comet, and is typical of the reduced images. The comet's coma extends very little, if at all, into the lower 50 rows of the image.

Much difficulty was encountered in disentangling the effects of poor seeing at the end of the evening from light loss due to extinction in the comparison stars. To circumvent these difficulties, we determined the extinction coefficient using only data prior to 7.24 UT (92 min post-impact), before the seeing degraded and the airmass exceed 6. Despite the difficulties in obtaining good comparison star data we were able to use U0750-0819673 (hereafter Star 4) shown in Fig. 3, to extract the R-band extinction coefficient on the night of impact. This star is listed in the USNOA catalog as having an R-band magnitude of 14.5 and a B-band magnitude of 16.0. The coordinates of Star 4 are listed as RA and Declination: 13:37:54.986, -09:35:23.03 (J2000).

We determined a value of 0.076 ± 0.010 mag/airmass for our extinction coefficient, by performing a linear least-squares fit (following Press et al. (1992)) to the instrumental magnitude vs. airmass of Star 4. Normally a very large aperture is used when determining the extinction coefficient to limit the light loss outside the aperture. For these observations we were forced to use both a small aperture and narrow annulus to measure the star and sky brightnesses because of the steep non-linear gradient in the coma light. We found that the best results were obtained with an aperture of 13 pixels ($10.4''$) and an annulus spanning 14–18 pixels. We could not simply use the mode of the bottom 50 rows of our image because Star 4, at closest approach to the comet, was well within the coma.

An exhaustive 512 day exploration of the extinction coefficients at MLO was undertaken from 1984 April to 1991 March (Ronald J. Angione, private communication). Fig. 4 shows the extinction coefficient determined from Angione's study along with the value obtained in our work using the method described above, where the mean extinction values for June and July are shown with the filled square and filled diamond respectively. Angione's study was performed with a series of narrow-band filters with a FWHM of 75 Å, none of which closely match the central wavelength of the Kron R-band filter. However, it can be seen in Fig. 4 that our determination of the extinction for the R-band filter on the night of impact is consistent with the mean values found by Angione.

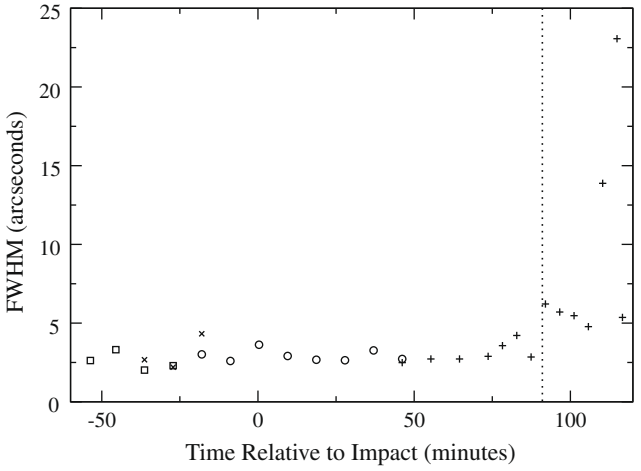

Fig. 1. The FWHM of the seeing based on four comparison stars. The four stars are shown with different symbols, with some overlap to indicate the consistency of the measurements. The dotted line at 90 min post-impact denotes the time when the seeing significantly degraded.

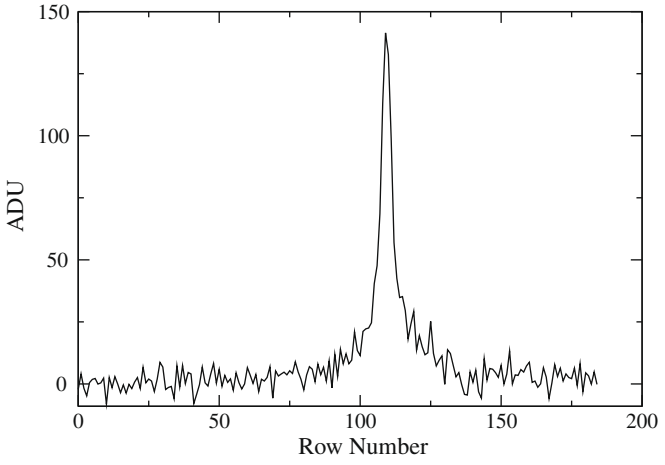

Fig. 2. A slice from a single 4-s calibrated image of Comet 9P/Tempel 1. This slice was taken from the 89th column of the image (through the comet) and illustrates the result of background subtraction technique using the bottom 50 rows of the image.

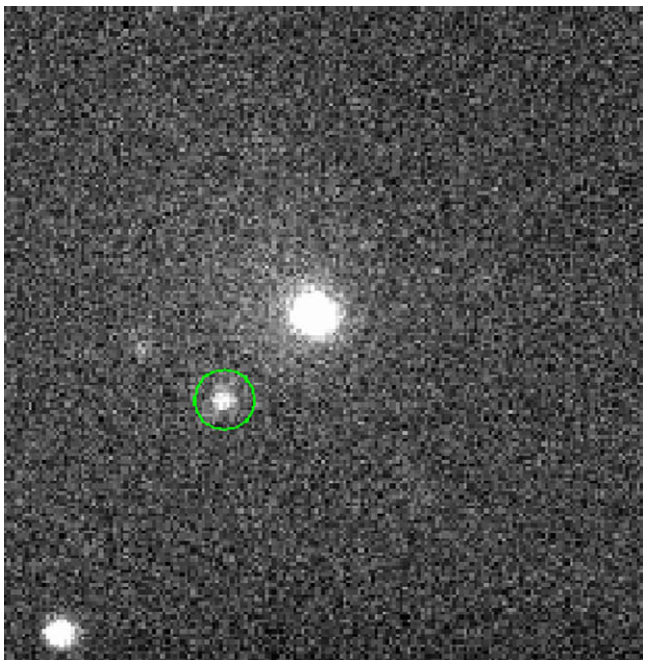

Fig. 3. A single 4 s exposure of Comet 9P/Tempel 1 shown with our main comparison star "Star 4" (circled). The image was taken at 07:04:44 UT, approximately 73 min post-impact and is typical of the short-exposure CCD images obtained at MLO on the night of impact. The FOV is $2' \times 2'$; north is to the right and east is to the top.

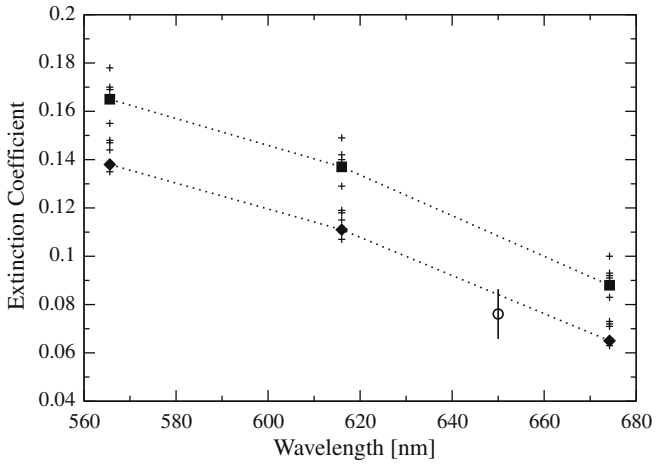

Fig. 4. The mean extinction for Mt. Laguna from solar radiometer measurements based on a study of extinction from 1984 April to 1991 March. The mean monthly values for the narrow-band filters used in the study are shown with plus symbols, and specifically, the mean extinction values for June and July are shown with the filled square and filled diamond. Our R-band extinction coefficient determined for the night of 2005 July 4 UT is shown as a circle.

Finally, we checked the uncertainties in the fluxes, as derived via the IRAF calibration process, with the observed rms scatter in a 22-min section of the pre-impact light curve from 05:30:00 UT until the time of impact. The IRAF error bars, based mostly on Poisson statistics, underestimated the actual scatter by a factor of 3.136. Thus we scaled all the error bars by this amount to get our final uncertainties. With this process, a linear fit to the pre-impact light curve yields a reduced χ^2 of unity. We note in passing that the 64 min of pre-impact flux is not completely constant; it contains a very slight decline, which we speculate to be caused by the rotation of the comet.

In addition to the MLO observations, we examined the light curve of (Barber et al., 2007), produced from the CCD guide camera images on the United Kingdom Infrared Telescope (UKIRT) that is normally used to guide the telescope. A $1.8'' \times 1.8''$ square aperture was used and the R-band light curve was normalized to the pre-impact level. This is a revised version of light curve shown in Fig. 5 of Meech et al. (2005); a full analysis is presented in (Barber et al., 2007). In this high signal-to-noise, high time-resolution light curve, the comet increased in brightness by a factor of 11.1. We created empirical uncertainties for these data by computing the rms scatter about a linear fit to short segments of the light curve. There are two distinct sections of data, those before and those after 11 min post-impact. For the first section we estimate the average uncertainty to be ±0.040 relative flux units, and ±0.142 for the second section; we assign these uncertainties to all data in the corresponding sections.

3. Light curve analysis

The MLO light curve of Comet 9P/Tempel 1 has a variety of morphologies in different sized apertures. This behavior can be seen in Fig. 5, which shows the light curves for $1.6''$, $8.0''$ and $16.0''$ radius apertures. The time of impact is marked by a rapid rise in flux which lasts just over 20 min, depending on aperture size. In the smallest aperture we used, 2 pixel radius ($1.6''$), the flux peaks ~50 min post-impact, then drops to nearly the pre-impact level by the end of the observing window. In the largest aperture measured, 20 pixel radius (16 arcs^{-1}), the flux continues to slowly increase after the initial rapid rise. The total R-band change in brightness, from pre-impact to peak, was a factor of 5.4 in the $1.6''$ aperture, 2.2 in the $8.0''$ aperture, and 1.7 in the $16.0''$ radius aperture. (The relative contribution of the light from the impact is diluted by the coma in the larger apertures.)

3.1. Short-timescale variations

The MLO light curve exhibits many short-timescale (~min) variations. Such rapid fluctuations could be due to a variety of interesting phenomena (e.g., continued out-gassing from the crater, small explosive sublimation events, fall-back of rocky ejecta debris onto the comet nucleus, illumination of a relatively small number of large, irregular-shaped, tumbling debris fragments, etc.). Interestingly, the light curve in the smallest apertures (see Fig. 5) shows excess rapid variance that is correlated with the brightening. This extra scatter is not seen in the larger apertures,

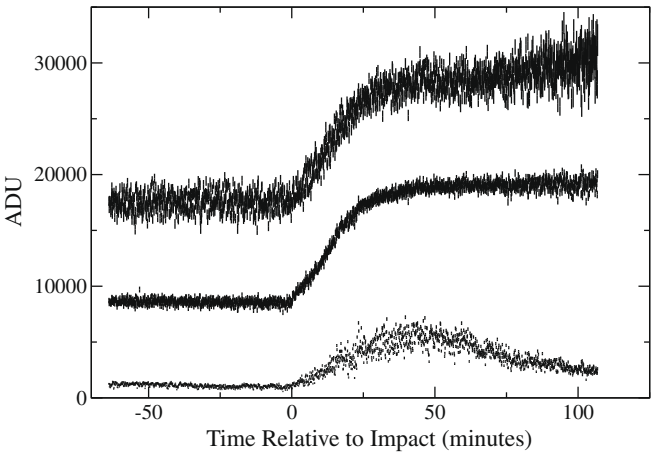

Fig. 5. The MLO R-band Deep Impact event light curve of Comet 9P/Tempel, through $1.6''$, $10.0''$ and $16.0''$ radius apertures (from bottom to top).

suggesting that it may be an instrumental artifact. But neither is it seen in the pre-impact section of the light curve, suggesting it is intrinsic to the comet (but perhaps confined to a region close to the nucleus).

To see if these short timescale variations are real, we compared the MLO 1.6″ aperture time series with the UKIRT light curve. To be able to see small variations, the light curves were first smoothed with a 21-point wide acausal Savitzky–Golay filter to filter out the highest frequency (white) noise (Press et al., 1992). Sections of the two smoothed light curves are shown in Fig. 6. A visual comparison of the two data sets shows no short-timescale correlation between the two data sets. This indicates that these fast variations are probably not associated with the activity of Comet 9P/Tempel 1 and are simply a result of sampling and seeing noise. We therefore focused our investigation on variations at longer timescales (few minutes and longer), where there is good correlation between our data set and others acquired during the impact event.

3.2. IRTF comparison

Fernández et al. (2007) collected approximately 26 min of spectroscopic data of Comet 9P/Tempel 1 on SpeX, a medium-resolution 0.8—5.4 μm spectrograph mounted on NASA's Infrared Telescope Facility (IRTF). Their spectra were then converted into effective JHK photometry. Their light curve shows a constant pre-impact flux that is followed by a rapid brightening in the first minute. The flux continues to increase at a more modest rate for the duration of the data set, but not at a constant rate (Fernández et al., 2007). Their light curves suggest changes in slope at 4 min and 9 min post impact.

For the analysis of the MLO data we used the photometry through an 8 $arcs^{-1}$ radius aperture because it had the best signal to noise ratio. The flux remains constant until 0.3 min (18 s) post-impact, and then a very rapid rise in flux lasting ~min takes place. During the first minute the flux increased by 0.093 ± 0.022 of the pre-impact level. Fig. 7 shows this rise and the first 16 min of the post-impact light curve.

Following Fernández et al. (2007), we have analyzed our data in a piece-wise linear fashion. Identical time intervals from Fernández et al. (2007) were adopted and we measured the slope for three sections of the rising light curve as we attempted to produce a figure similar to their Fig. 2. The three sections fell between 1–4 min, 4–8 min, and 9–15 min post-impact. A slope of 0.036 ± 0.010 of pre-impact flux per minute was found for the 1–4 min interval. The 4–8 min interval has a slope of 0.034 ± 0.010 of pre-impact flux per minute. The final interval, 9–15 min had a slope of 0.053 ± 0.008 of pre-impact flux per minute. The nearly identical slopes of the first two intervals suggests that there is no pivot at 4 min in the MLO data.

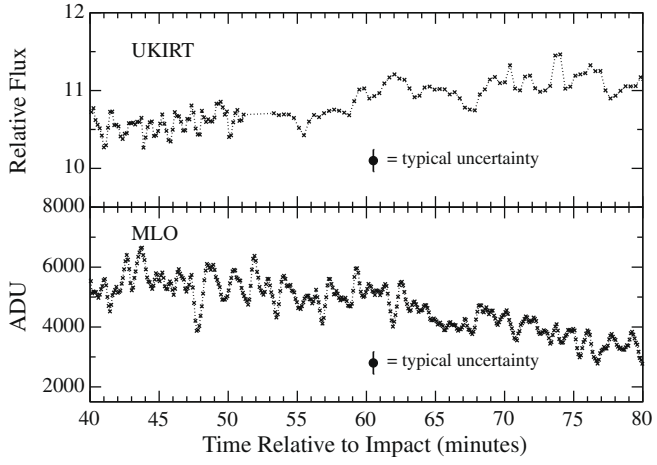

Fig. 6. A 40-min segment of the light curves from UKIRT (top panel) and the 1.6″ aperture MLO (bottom panel), after smoothing each with a Savitzky–Golay filter. A comparison of the fluctuations seen in the two light curves shows they are uncorrelated and almost certainly due to noise.

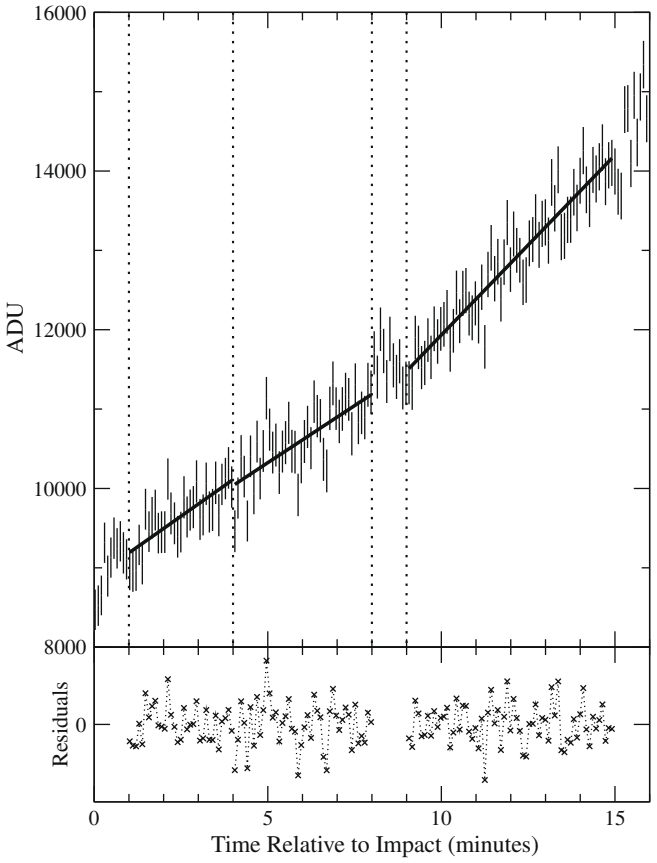

Fig. 7. Linear fits to the early post-impact MLO light curve, using the 8.0″ radius aperture photometry. The dotted lines mark three time intervals from Fernández et al. (2007): 1–4 min post-impact, 4–8 min post-impact, and 9–15 min post-impact. The first two intervals do not have any noticeable change in slope.

Changes in slope in the light curve were further investigated by re-determining the pivot point in the MLO data. The pivot point was stepped though the light curve in time and the χ^2 of linear fits on either side of the pivot were summed to obtain a χ^2_{total}. The pivot point is then the time that gives the lowest χ^2_{total}. Fig. 8 shows the results of the χ^2 fitting. Care was taken to insure continuity at the pivot.

A significant pivot was found at $9.16^{+0.55}_{-0.42}$ min post-impact. A slope of 0.034 ± 0.001 of pre-impact flux per minute was determined for the first interval from 1 to 9.16 min post-impact. The second interval, from 9.16 to 15 min, has a slope of $0.053^{+0.002}_{-0.003}$ of pre-impact flux per minute. The change in slope at 4 min post-impact found by Fernández et al. (2007) is not present in our data. This discrepancy may result from the different band-passes for the light curves. The SpeX observations, in the near-IR portion of the spectrum, are more sensitive to smaller grain sizes than the R-band observations from MLO and longer wavelengths will have lower optical depths than shorter wavelengths for a given column density of dust. The fragmentation of icy grains in the post-impact coma would change the size distribution of grains and effect the observed light curves differently because of their dependence on grain size and differences in optical depth.

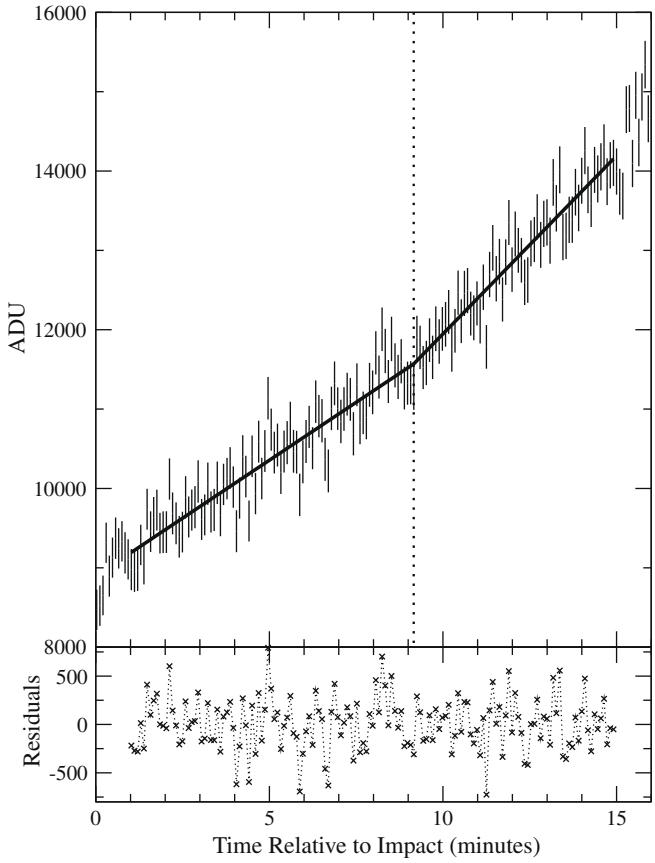

Fig. 8. A two-line fit to the early post-impact MLO light curve. The pivot point is located at 9.16 min post-impact and is marked with a vertical dotted line. Compare with Fig. 7.

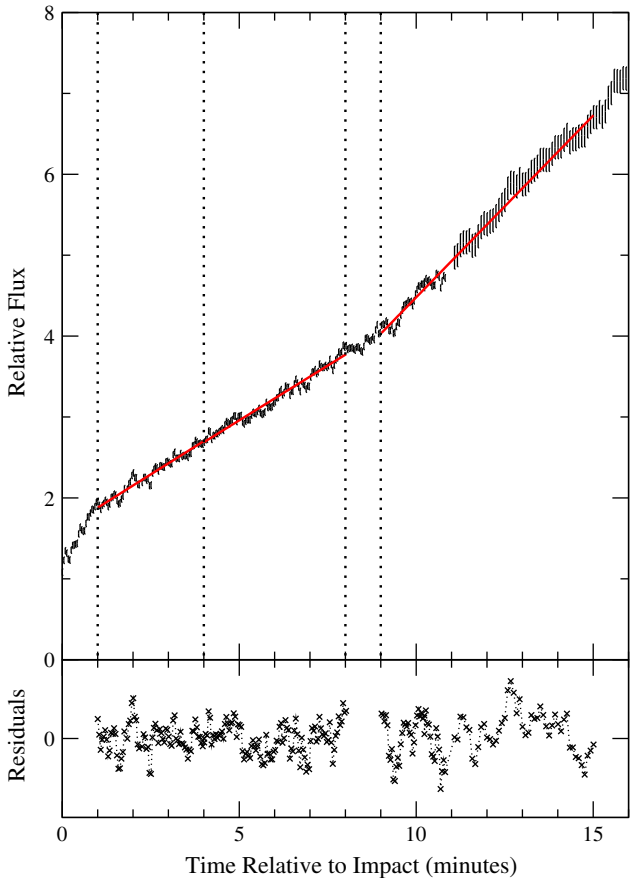

Fig. 9. Linear fits to the early post-impact UKIRT light curve. The dotted lines mark three time intervals from Fernández et al. (2007). Compare with Fig. 7.

3.3. UKIRT comparison

We analyzed the UKIRT data in an identical fashion to that of the MLO data. Linear functions were fit to the UKIRT data over the same time intervals used by Fernández et al. (2007). Fig. 9 shows the UKIRT light curve from 0 to 16 min post-impact along with the fits. For the interval from 1 to 4 min, we measured a slope of 0.274 ± 0.009 of the pre-impact flux level per minute. A nearly identical slope is found for the 4–8 min interval 0.272 ± 0.009 of the pre-impact flux level per minute. For the third and final interval, from 9 to 15 min post-impact, the slope is 0.449 ± 0.018 of the pre-impact flux level per minute. We conclude that there is no slope change in the UKIRT data at 4 min post-impact, but that a change in the rate of brightening does occur sometime between 8 and 9 min post-impact. Note that the values of the slopes are much larger than the corresponding values for the MLO light curve: this is because the different seeing conditions and aperture sizes used result in very different relative contributions of the ejecta plume light to the "background" coma. In the MLO data, no coma background was removed; only the sky level was subtracted. In the UKIRT data, the background from ~1.8″ around the comet was removed, which includes the coma. Thus the light from the dust ejecta in the UKIRT data contributes far more than in the MLO data. (This is also why the relative increase in brightness is so different between data sets.)

Following the same procedure as for the MLO light curve, we found a pivot point of $9.23^{+0.06}_{-0.11}$ min post-impact. From 1 min to the pivot point a slope of 0.272 ± 0.002 pre-impact flux level per minute is present. After the pivot, the slope changes to $0.460^{+0.008}_{-0.009}$ of the pre-impact flux per minute. These linear fits are shown in Fig. 10 and the slopes are tabulated in Table 1.

The slope of the UKIRT light curve increases by a factor of 1.5 at the pivot at 9.2 min post-impact. For the MLO light curve the slope increases by a factor of 1.7, also at 9.2 min post-impact. The agreement of these pivot times and slope changes gives us confidence that this is a real event. Furthermore it appears that there may be a slope change in the Fernández et al. (2007) observations around 9 min.

4. Ejecta velocity

Fig. 11 shows the light curve in a variety of aperture sizes ranging from 1.6″ to 16.0″, in ascending order from the bottom. The light curves have been smoothed with a Savitzky–Golay filter to reduce high frequency noise (Press et al., 1992) yet preserve the shape. If the R-band flux simply increased post-impact, the ratio of light curves in different apertures would remain mostly constant at all times. Instead, the light curves in the small apertures peak at ~45 min then drop off, while in the large apertures (>8″), the flux remains constant or continues to grow slightly throughout the duration of the observations. It is important to realize that the monotonic increase in the largest apertures indicates that the comet does continue to brighten for the duration of the observations; only in the smaller apertures is there a net decrease in flux. A peak, followed by a decrease in brightness is seen in several ground-based Deep Impact light curves (e.g. Mumma et al., 2005; Barber et al., 2007; Cochran et al., 2007). As seen in our data, the smaller the aperture used in the photometry, the earlier the peak and faster the decay. We interpret the drop-off in flux in the smaller apertures as a result of the bright expanding ejecta moving beyond the edge of the aperture.

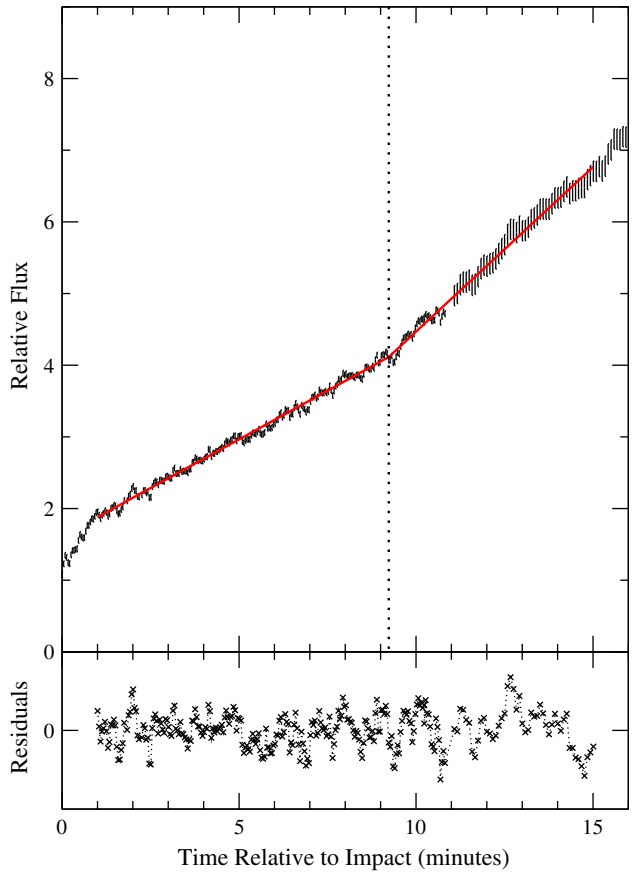

Fig. 10. A two-line fit to the UKIRT light curve. The pivot point is located at 9.23 min post-impact and is marked with a vertical dotted line. Compare with Figs. 8 and 9.

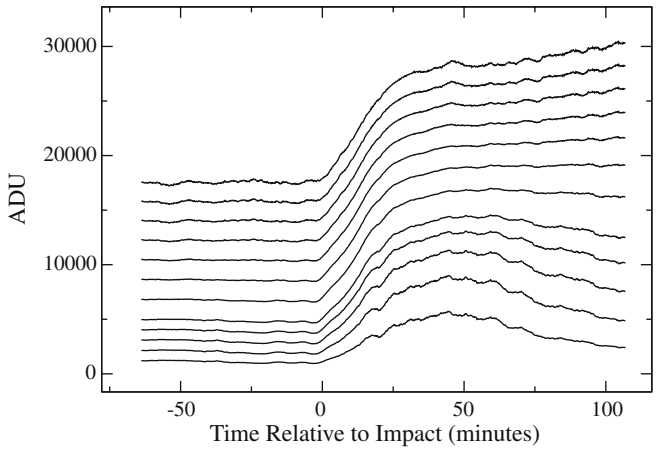

Fig. 11. R-band light curves from MLO on the night of July 4 UT in several apertures. The flux through 1.6, 2.4, 3.2, 4.0, 4.8, 6.4, 8.0, 9.6, 11.2, 12.8, 14.4 and 16.0 arcs radius apertures are shown in ascending order from the bottom. The light curves have been smoothed with a Savitzky–Golay filter. Notice that the light curves in the smaller apertures peak then decline while the flux continues to increase in the larger apertures.

Estimates of the expansion speed of the ejecta range from 0.18 to 0.51 km s^{-1} (e.g. Bonev et al., 2007). At these speeds the bulk of the ejecta would have expanded beyond a 1-arcs radius aperture within 1 h. This agrees with the timescale of the peaks (∼45 min) seen in the 1.6″ aperture light curve show in Fig. 11. The ejecta, however, will not extend to radii greater than about 6″ within the duration of the observing window; the larger aperture light curves do not show a peak and decline, consistent with this interpretation.

The decline in the light curves starts around 45–50 min post-impact. As seen in Fig. 1 the seeing, although not good, remained fairly constant through this time, and started to degrade around 90 min post-impact. This argues that the drop in the light curves is not caused by loss of light from the smaller apertures. In addition, because the comet/coma is somewhat spatially extended (larger than the seeing psf), slight changes in seeing would tend to scatter light both into and out of the very smallest apertures, resulting in less light-loss than if the source was point-like. The FWHM of the comet just prior to impact was 4.23″ versus 2.74″ for a stellar image.

Assuming the drop in flux is due to the ejecta extending beyond the smaller apertures, then the times of peaks of the light curves for increasing-sized apertures should provide an estimate the expansion velocity of the ejecta. Each ∼0.8″ pixel corresponds to a linear size of ∼519 km at the distance of the comet at the time of impact, giving the physical scale of the aperture. The radius of each aperture in kilometers divided by the peak time for that aperture gives a rough estimate of the expansion velocity. This straightforward method is complicated by the noisy and broad-peaked light curves that do not provide a precise time of maximum. Furthermore, we do not know of a functional form to fit to the light curve. Nevertheless, we were able to reasonably estimate the times of peaks by fitting polynomials via least squares, using times of 10–75 min post-impact (similar results we obtained when we fit times 1–90 min). Polynomials of order 5–6 gave the best fits in a reduced χ^2 sense, though higher order fits (up to order 11 or 12) gave acceptable fits to the eye (i.e., before beginning to be so flexible as to fit the noise). The range of peak times is provided in Table 2, along with the physical size of the apertures, and the estimated velocities. The uncertainties listed include a 4.6% uncertainty in the CCD plate scale for the 1-m telescope. This results in an expansion velocity of 0.35—0.99 km s^{-1}. Since the uncertainties used are estimates, not $1-\sigma$ confidence intervals, we simply quote a range of velocities. Alternatively, using centroids (geometric center for 10–75 min post-impact) instead of the peaks yields a similar velocity of 0.44—0.62 km s^{-1}, but the centroid is very sensitive to the chosen endpoints.

This value is roughly consistent with the wide range of other published values for the dust expansion velocity: 0.18 ± 0.03–0.51 ± 0.06 km s^{-1} (Bonev et al., 2007), 0.11 km s^{-1} (Küppers et al., 2005), 0.20 ± 0.02 km s^{-1} (Meech et al., 2005) and 0.13—0.23 km s^{-1} (Schleicher et al., 2006). Furthermore, Cochran et al. (2007) estimate an expansion of >0.51 km s^{-1} based on the CN molecule. Although our result does not further constrain the ejecta velocity, the consistency supports the idea that the loss of light in small apertures is due to the ejecta moving beyond the edge of the photometric apertures.

Table 1
Slopes for the rising MLO and UKIRT light curves. The units are in pre-impact flux per minute. The post-impact pivot times are $9.16^{+0.55}_{-0.42}$ min for the MLO and $9.23^{+0.06}_{-0.11}$ min for the UKIRT observations.

Data set	Slope		
	1–4 min	4–8 min	9–15 min
Slope relative to pre-impact flux			
MLO	0.036 ± 0.010	0.034 ± 0.010	0.053 ± 0.008
UKIRT	0.274 ± 0.009	0.271 ± 0.009	0.449 ± 0.018
	Pre-pivot	Post-pivot	
MLO	0.034 ± 0.001	$0.053^{+0.002}_{-0.003}$	
UKIRT	0.272 ± 0.002	$0.460^{+0.008}_{-0.009}$	

Table 2
Aperture radii, time of peak, and velocity estimate.

Aperture (pix)	Aperture (km)	Time of peak (minutes post-impact)	Velocity (km s^{-1})
Dust ejecta velocity estimates			
2	977.25–1070.6	44.6–46.3	0.352–0.400
3	1465.9–1605.9	45.0–48.2	0.507–0.595
4	1954.5–2141.2	49.2–50.6	0.644–0.725
5	2443.1–2676.6	51.5–52.7	0.773–0.866
6	2931.8–3211.9	54.2–55.0	0.888–0.988

The increasing velocities with aperture indicates a systematic problem, perhaps due to a change in optical depth in addition to the ballistic motion of the dust cloud. While it is possible that the time of peak is correlated with the time at which the expanding ejecta becomes optically thin and the flux begins to drop, the ejected material can have a range of velocities such that the faster material exits our smaller apertures at a different rate than the slower material. So while the derived velocities are consistent with other published estimates, they should be treated with caution.

5. Discussion

The temporal evolution of the increasing brightness of the ejecta involves many factors including the optical depth of the ejecta, the geometry of the ejecta cloud and the viewing angle of the observer, the location of the Sun relative to the comet, and even the chemical and physical evolution of the ejecta. All of these factors can influence the amount of sunlight scattered to Earth by the ejecta plume. The type of function used to model the light curve of a comet impact is at this stage ad hoc.

The increase in brightness of the ejecta cloud is highly dependent on its optical depth. We know that the ejecta cloud remained optically thick for at least the first 15 min after the impact because the impact site was obscured from the view of the flyby spacecraft (A'Hearn et al., 2005) and the ejecta cast a shadow onto the comet. At some point, a transition to an expanding cloud of optically thin material should take place. The brightness should remain mostly constant after the ejecta becomes optically thin because even though the volume of the cloud is growing with time, the total mass of material and therefore the total scattering cross-section will remain mostly constant, assuming the grain sizes also remain constant. This is only true if the entire cloud remains within the radius of the photometric aperture. This could explain the lack of a peak seen in the light curves measured through large apertures in the MLO light curves.

In contrast, the evolution of the light curve is more complicated while the ejecta is optically thick. To first order, the shape of the ejecta plume is conical. In their best model Schleicher et al. (2006) find an Earth–comet–plume angle of 70°. Therefore, Earth-based observers see the ejecta plume with a triangular face towards Earth and the base, or widest part, of the cone nearly edge-on. The Earth–comet–Sun angle of 104° at the time of impact puts the Sun at a 34° angle with respect to a vector normal to the base of the conic plume (Blume, 2005). Therefore, from an Earth-perspective, the plume is illuminated mostly along the base of the cone down to a depth of $\tau \sim 1$.

Initially, assuming the material is optically thick and cone-shaped, a strip of material along the base of the cone would be the only material not in shadow and able to scatter light back to Earth. As the ejecta cloud grows, this edge would grow linearly with time and hence the observed brightness would also increase linearly with time. Therefore, assuming the outflow velocity is constant and there are no other factors such as icy grain sublimation and/or fragmentation involved, the rate of increasing brightness as a function of time should tell us about the geometry of the ejecta and the optical depth in the following manner:

$$f(t) \propto \begin{cases} \text{constant} & \text{if optically thin} \\ t & \text{if optically thick edge} \\ t^2 & \text{if optically thick area} \end{cases} \quad (1)$$

As seen in Section 3, the initial rise is well-fit with a linear function of t. The reduced χ^2 for a linear fit is statistically better than a quadratic fit, for both sections of data: 1–9.2 min and from 9.2 to 15 min post-impact. This suggest that the ejecta was optically thick at these times (for at least the first ~15 min, and perhaps to 25 min post-impact) and that mainly the edge of the ejecta is scattering sunlight back to Earth. The other factors such as the sublimation of icy grains may be having an effect on the behavior of the light curve. They would increase the effective scattering surface of the ejecta cloud, which would increase the rate of brightening. Such an increase in the rate of brightening is seen after 9.2 min post-impact.

Water ice was found in the spectra of the Deep Impact ejecta (Lisse et al., 2006). The chemical and physical evolution of the ejected particles will be effected by the sublimation of dust–ice conglomerates, icy grains. Spectral analysis by DiSanti et al. (2007) shows a delayed increase in parent volatiles in the post-impact Deep Impact spectra, with a sharp increase in the abundances of water and other parent volatiles at a post-impact time of 25 min, suggesting a change in optical depth at this time. It has been suggested that the kinetic energy of the impactor, 1.9×10^{10} J (A'Hearn et al., 2005), was insufficient to completely vaporize the total amount of water ice ejected. This would suggest a time delay in the sublimation of icy grains within the ejecta. The sublimation of icy grains would affect the size distribution and density of dust in the ejecta cloud in such a way as to increase the scattering cross-section of the ejecta cloud. When a large icy grain breaks apart, the many smaller daughter grains have a larger effective cross-section than the large parent grain.

6. Summary

The R-band impact light curve shows a near constant pre-impact flux until about 18 s post-impact, at which time a dramatic increase occurs: a change of 9.3 ± 2.2% occurs in 1 min in an 8.0″ radius aperture. The light curve then shows a slower linear increase with a slope of 3.5% per minute until 9.2 min post-impact, when a transition occurs and the slope increases by a factor of 1.5. The flux continues to increase before leveling off at ~50 min post-impact. This leveling off most likely corresponds to the time at which the ejecta cloud began to become optically thin, but may also be influenced by other factors such as grain sublimation and fragmentation. In larger apertures the flux plateaus or continues to grow slightly for the duration of the observations. The flux in apertures <8.0″ reach a peak at ~50 min post-impact then decline back towards the pre-impact level. Because the comet and ejecta are not point-sources, the relative increase in flux depends on the aperture in which the flux is measures. In our images, the peak brightness increase ranged from a factor of 5.4 in the smallest aperture measured (1.6″ radius) to a factor of 1.7 in the largest (16.0″ radius).

The change in slope at ~7–9 min after the impact is present in several datasets (Meech et al., 2005). Although the overall behavior is similar between independent observations, there may be subtle differences in the slope and the locations in time when the slopes change that might be attributed to the differences in band-pass and aperture size between the data sets. The similar morphology between the independent MLO and UKIRT datasets causes us to believe that the change at 9.2 min is not instrumental and that some physical phenomena is responsible. The changes in slope during the rise of

the light curve have been attributed to varying rates of ejecta production due to the impact, chemical and physical evolution of the ejecta particles, as well as the expansion of the ejecta cloud.

Two intervals, from 1.0 to 9.2 min and 9.2 to 16.7 min post-impact, were fit with linear and quadratic functions and the linear fit had a better reduced χ^2 in both cases. We interpret this change in slope to mean the expanding ejecta is optically thick during these intervals and that only an edge of the dust cloud is scattering sunlight back to Earth. The sublimation of icy grains in the ejecta is probably playing a role in shaping the light curve, and is probably responsible for the increase in slope at 9.2 min post-impact. Since we do not know how the rate of brightening caused by the sublimation of icy grains should depend on time, we can not say for sure if this is actually the cause of the increased rate of brightening.

For the smaller apertures in which the light curves exhibit a peak, the time of the peak increases as the aperture size increased. From this we estimate the expansion velocity of the ejected dust cloud to be 0.35—0.99 km s^{-1}, in good agreement with other published values of ~0.2—0.5 km s^{-1}. However, the lack of any peak in larger aperture light curves hints at a more complicated combination of multiple processes at work (change in optical depth, etc.). Until these processes can be better understood, caution should be taken when interpreting the light curve drop-off as simply due to bulk motion of the ejecta beyond the aperture.

Acknowledgments

We would like to acknowledge the work of Dr. Robert W. Leach of the SDSU CCD Laboratory for enabling the high-speed readout mode that made these observations possible. We thank Dr. Ronald Angione for providing us with his MLO extinction study, and also thank Mr. Merek A. Cherkow, an NSF REU student, for assisting with the observations at MLO on the night of the impact. We also thank the anonymous reviewers for their extremely valuable comments and insights that significantly improved both the content and presentation of this paper.

Data collection for this research was enabled by the HPWREN Project http://hpwren.ucsd.edu at the University of California San Diego under National Science Foundation Grants 0087344 and 0426879 to H.-W. Braun and F. Vernon.

References

A'Hearn, M.F., 1983. Photometry of Comets. In: Genet, R.M. (Ed.), Solar System Photometry Handbook. William-Bell, Inc., Richmond, pp. 3-1–3-33.
A'Hearn, M.F., and 32 colleagues, 2005. Deep Impact: Excavating Comet Tempel 1. Science 310, 258–264.
Barber, R.J., Miller, S., Stallard, T., Tennyson, J., Hirst, P., Carroll, T., Adamson, A., 2007. The United Kingdom Infrared Telescope Deep Impact observations: Light curve, ejecta expansion rates and water spectral features. Icarus 187, 167–176.
Blume, W.H., 2005. Deep Impact mission design. Space Sci. Rev. 117, 23–42.
Bonev, T., and 19 colleagues, 2009. Deep Impact as a World Observatory Event: Synergies in Space, Time, and Wavelength. Springer, Berlin, pp. 177-184.
Cochran, A.L., Jackson, W.M., Meech, K.J., Glaz, M., 2007. Observations of Comet 9P/Tempel 1 with the Keck 1 HIRES instrument during Deep Impact. Icarus 187, 156–166.
DiSanti, M.A., Villanueva, G.L., Bonev, B.P., Magee-Sauer, K., Lyke, J.E., Mumma, M.J., 2007. Temporal evolution of parent volatiles and dust in Comet 9P/Tempel 1 resulting from the Deep Impact experiment. Icarus 187, 240–252.
Fernández, Y.R., Lisse, C.M., Kelley, M.S., Dello Russo, N., Tokunaga, A.T., Woodward, C.E., Wooden, D.H., 2007. Near-infrared light curve of Comet 9P/Tempel 1 during Deep Impact. Icarus 187, 220–227.
Küppers, M., and 40 colleagues, 2005. A large dust/ice ratio in the nucleus of Comet 9P/Tempel 1. Nature 437, 987–990.
Lisse, C.M., and 16 colleagues, 2006. Spitzer spectral observations of the Deep Impact ejecta. Science 313, 635–640.
Marsden, B.G., 1983. Catalog of Cometary Orbits, first trade ed. Enslow Publishers, Hillside, NJ.
Meech, K.J., and 208 colleagues, 2005. Deep Impact: Observations from a worldwide earth-based campaign. Science 310, 265–269.
Mumma, M.J., and 13 colleagues, 2005. Parent volatiles in Comet 9P/Tempel 1: Before and after impact. Science 310, 270–274.
Press, W.H., Teukolsky, S.A., Vetterling, W.T., Flannery, B.P., 1992. Numerical Recipes in FORTRAN, second ed.. The Art of Scientific Computing University Press, Cambridge.
Schleicher, D.G., Barnes, K.L., Baugh, N.F., 2006. Astron. J. 131, 1130–1137.
Sugita, S., and 22 colleagues, 2005. Subaru telescope observations of Deep Impact. Science 310, 274–278.
Warner, E., Redfern, G., 2005. Deep Impact: Our first look inside a comet. Sky & Telescope 109, 40–44.